The Astrophysical Journal, 763:39 (7pp), 2013 January 20 doi:10.1088/0004-637X/763/1/39

GRAVITATIONAL FRAGMENTATION IN GALAXY MERGERS: A STABILITY CRITERION

Andrés Escala, Fernando Becerra, Luciano del Valle, and Esteban Castillo
Departamento de Astronomía, Universidad de Chile, Casilla 36-D, Santiago, Chile
Received 2012 February 7; accepted 2012 November 27; published 2013 January 4

ABSTRACT

We study the gravitational stability of gaseous streams in the complex environment of a galaxy merger, because mergers are known to be places of ongoing massive cluster formation and bursts of star formation. We find an analytic stability parameter for the case of gaseous streams orbiting around the merger remnant. We test our stability criterion using hydrodynamic simulations of galaxy mergers and obtain satisfactory results. We find that our criterion successfully predicts the streams that will be gravitationally unstable to fragmentation into clumps.

Key words: galaxies: formation – galaxies: interactions – galaxies: star clusters: general

Online-only material: color figures

1. INTRODUCTION

Galaxy mergers are believed to be not just common events in the universe but also fundamental pieces in the evolution of galaxies since they trigger bursts of star formation (Larson & Tinsley 1978; Sanders & Mirabel 1996) and they are a key ingredient in the formation of elliptical galaxies and bulges (Toomre & Toomre 1972; Mihos & Hernquist 1994, 1996; Kazantzidis et al. 2005; Di Matteo et al. 2007). More recently, it has also been found that many interacting and merging galaxies are places of current massive cluster formation (Schweizer & Seitzer 1998; Mengel et al. 2008).

Standard numerical simulations of galaxy mergers that include gas (Mihos & Hernquist 1994; Barnes & Hernquist 1996; Kazantzidis et al. 2005; Cox et al. 2006; Di Matteo et al. 2007) have been able to reproduce the observed starbursts which occur during the merging process on nuclear gaseous disks. However, they intentionally avoid fragmentation through high minimum temperatures and large gravitational softening lengths and therefore, fail to reproduce formation of massive star clusters. Only recently have simulations had the resolution required to study gas fragmentation on at least large scales (Bournaud et al. 2008; Saitoh et al. 2009; Teyssier et al. 2010; Matsui et al. 2012). In those simulations, massive star clusters are indeed formed by gas fragmentation into collapsing clumps and it is therefore relevant to have a criterion for gravitational instabilities in such a complex environment.

The study of gravitational stability of fluids started with the work of Jeans (1902) for a uniform, infinite, and isothermal gas, and was later extended by Bonnor (1956) and Ebert (1955) for a finite and spherically symmetric fluid, a rotationally supported fluid (Toomre 1964; Goldreich & Lynden-Bell 1965), and a magnetized fluid (Chandrasekhar & Fermi 1953), among others. In this paper we study the stability of gaseous streams in the complex environment of a galaxy merger by means of smoothed particle hydrodynamics (SPH) numerical simulations.

The paper is organized as follows. We start in Section 2 with a discussion of the physical processes relevant to stabilizing gaseous streams in galaxy mergers and provide analytical estimates for a stability criterion. Section 3 continues with a discussion of the setup of the galaxy mergers simulations and the resolution needed to resolve gravitational instabilities in galaxy mergers. In Section 4 we test the stability criterion by performing hydrodynamical simulations of galaxy mergers with the resolution discussed in Section 3. Finally, we summarize the results of this work in Section 5.

2. BASIC PHYSICAL INGREDIENTS: GAS PRESSURE AND MOTION

High-resolution simulations of galaxy mergers have generally found galactic streams such as tails and bridges at large scales and more complex ones on inner kiloparsec scales where collapsing clumps are ubiquitous features formed by gravitational instabilities. However, no gravitational instability criterion for the complex and irregular case of gaseous streams in a galaxy merger has been found.

The most basic physical processes that could overcome gravity in the absence of magnetic and other fields are gas pressure and motion. Since gas pressure is isotropic and does not depend on the geometry of the fluid, only on its local density and temperature, its stabilizing role on small scales is the same as in a fluid with a regular geometry (i.e., with a given symmetry). On the other hand, the motion of streams is much more complex and is not constrained to a single plane but in central regions (inner kpc, where the bulk of the star and cluster formation occurs) it is characterized by streams orbiting around the center of mass of the newly formed system.

A simple and useful approach is to model individual streams as a piece of a rotating annulus. In such a case, it is known from vector calculus that the rotational component of motion is well described by an angular frequency, which is defined relative to an origin O of the coordinate system in which we describe the motion:

$$\boldsymbol{\Omega}_{\rm O} = \frac{\boldsymbol{r}\times\boldsymbol{v}}{\boldsymbol{r}\cdot\boldsymbol{r}} = \frac{\boldsymbol{r}\times\boldsymbol{v}}{r^2} = \hat{r}\times\frac{\boldsymbol{v}}{r}, \tag{1}$$

where $\boldsymbol{r} = r\,\hat{r}$ and $\boldsymbol{v}$ are, respectively, the position and velocity vectors.

Under this approximation, the stability of individual streams is a very similar problem to the stability of annuli in a rotating sheet, with the difference that the streams in the merger case do not belong to the same plane ($\boldsymbol{\Omega}_{\rm O}$ of individual streams can have a different magnitude and direction). In such a case, from dimensional analysis it is straightforward to conclude that results from standard gravitational instability analysis in a rotating sheet (Toomre 1964; Goldreich & Lynden-Bell 1965; Binney & Tremaine 2008) should still be valid for a given stream: there is a range of unstable length scales limited on small scales by

thermal pressure (at the Jeans length $\lambda_{\rm Jeans} = C_{\rm s}^2/G\Sigma_{\rm gas}$) and on large scales by rotation (at the critical length set by rotation, which for this case can be defined as $\lambda_{\rm rot} \equiv \pi^2 G\Sigma_{\rm gas}/|\mathbf{\Omega}_{\rm O}|^2$). All intermediate length scales are unstable, the most rapidly growing mode has a wavelength $2\,\lambda_{\rm Jeans}$, and the most unstable mode has a wavelength $\lambda_{\rm rot}/2$. Only a combination of pressure and rotation can stabilize the stream; this occurs when the range of unstable wavelengths shrinks to zero (i.e., the two scales are comparable), i.e., for $\lambda_{\rm Jeans} \geqslant (q/\pi)^2\,\lambda_{\rm rot}$ (Escala & Larson 2008). Therefore a stream will be stable if

$$|\,\boldsymbol{Q}_{\rm O}| \equiv \frac{C_{\rm S}\,|\mathbf{\Omega}_{\rm O}|}{G\,\Sigma_{\rm gas}} \geqslant q, \qquad (2)$$

where $C_{\rm S}$ is the gas sound speed, $|\mathbf{\Omega}_{\rm O}|$ is the norm of the angular frequency vector, G is the gravitational constant, $\Sigma_{\rm gas}$ is the gas surface density, and q is a number of the order of unity. Otherwise, a stream will be unstable if $|\,\boldsymbol{Q}_{\rm O}| < q$.

It is important to point out that the concept of angular frequency depends on the origin of the coordinate system chosen to describe the motion and, contrary to the case of the rotating sheet, there is not an obvious single choice for all streams in a galaxy merger. This becomes relevant in Section 4 when we compare the results of this section with numerical simulations to test whether or not the stability criterion given by Equation (2) is valid. Our approach in Section 4 will be to check if, with a single origin of the coordinate system O, Equation (2) is able to predict the gravitational instability of the streams. This assumption will introduce changes in the value of the angular frequency and therefore in the determination of the value for the threshold q (this will be an average value for all streams). However, our aim is to have a simple criterion that can be easily applied by other authors and in such a case it is better to have a single $|\,\boldsymbol{Q}_{\rm O}|$ with an average fitting parameter q than to have a $|\,\boldsymbol{Q}_{{\rm O}\alpha}|$ and a q_α for each stream α.

In the case that all the streams are coplanar and orbit around the same point, we recover the standard Toomre Q parameter for a rotating sheet ($=C_{\rm S}\,\Omega/G\,\Sigma_{\rm gas}$; Toomre 1964), since now the direction of $\mathbf{\Omega}_{\rm O}$ and the origin O chosen to describe the motion is the same for all streams.

3. SIMULATIONS OF GRAVITATIONAL FRAGMENTATION IN GALAXY MERGERS

In the following, we perform a set of idealized numerical experiments aimed to test if the stability parameter (Equation (2)) successfully predicts the streams in a galaxy merger that will be gravitationally unstable to fragmentation into clumps. These experiments are constructed to be as simple as possible in order to guarantee that the gas fragmentation is only due to gravitational instabilities. For that reason, we use an isothermal equation of state instead of having a multiphase medium and we do not include any feedback processes from star formation and/or active galactic nuclei (AGNs) which will make the analysis more complex as it includes new sources that may trigger fragmentation. Without including this extra physics we cannot aim to have a realistic description of the interstellar medium (ISM), but it will be sufficient for our main purpose, which is to study the onset of gravitational instability at large scales in a galaxy merger.

The simulation consists of the merger of two equal-mass disk galaxies, and we let the two galaxies collide on a parabolic orbit with pericentric distance $R_{\rm min} = 7.35$ kpc. The simulations start with an initial separation of 49 kpc, where the separation distance is measured between the mass centers of the two galaxies and the initial inclination angle between the disk planes of the individual galaxies is 90°. The galaxies are initialized using the code GalactICS: in particular we use "Milky Way model A" (see Kuijken & Dubinski 1995 for details). In each galaxy model, we include a gaseous disk with the same exponential profile as the stellar component (Kuijken & Dubinski 1995) and with a total gas mass corresponding to 10% of the total stellar disk mass. The gas has an isothermal equation of state, $P = c_{\rm S}^2\,\rho$, where the sound speed is fixed at $c_{\rm S} = 12.8\,{\rm km\ s^{-1}}$, corresponding to a gas temperature of $\sim 2\times10^4$ K. At $t = 0$ the gaseous disk of each isolated galaxy is gravitationally stable. In our simulations, we use the following internal units: [Mass] $= 5.8\times10^{11}\,M_\odot$, [Distance] $= 1.2$ kpc and $G = 1$. The total number of particles is 420,000, 200,000 for sampling the gas, 120,000 for the dark matter halo, 80,000 for the disk component, and 20,000 for the bulge.

The simulations were evolved using the SPH code Gadget-2 (Springel 2005) up to a time $t = 160$ (in internal time units), which corresponds to a point where the galaxies are after their third (and final) pericentric passage and in which most of the gas (>80%) has been fueled to the central kiloparsec. Figures 1(a)–(d) show the evolution of the system at four times, $t = 32$ (a), 54 (b), 120 (c), and 136 (d), which correspond to before (a) and after (b) the first pericentric passage, the second pericentric passage (c), and at the third pericentric encounter of the galaxies (d). The ring/oval structures seen in Figures 1(a)–(c) are ubiquitous features found since early simulations of galaxy mergers (e.g., Schwarz 1984) and are believed to be tightly wound spirals that are the gas response to tidal forcing (e.g., Barnes & Hernquist 1996).

3.1. Minimum Gravitational Resolution

Before analyzing the stability of gaseous streams it is necessary to check that we have the gravitational resolution required to resolve the fragmentation of streams into collapsing clumps: for this reason we perform a convergence test. We restarted the original simulation with a gravitational softening length $\epsilon_{\rm soft} = 0.4$ at $t = 132$ and allowed $\epsilon_{\rm soft}$ to change at later times to 0.04, 0.02, 0.01, 0.008, and 0.006 in internal units.

Figures 1(e)–(h) show the evolution of the restarted simulation at a later time $t = 134$ in a region of radius 2 internal distance units (2.4 kpc) for different gravitational softening lengths: 0.4 (e), 0.04 (f), 0.01 (g), and 0.006 (h). Figures 1(e)–(h) show that as the softening length decreases we find more gas fragmentation until a point at which the resulting simulations converge. We find convergence of the results for $\epsilon_{\rm soft} \leqslant 0.01$ and for this reason we choose to use a gravitational softening length of $\epsilon_{\rm soft} = 0.01$ in the following section.

The convergence can be understood if we take into account that over 99.6% of the particles in such a region fulfill the condition $\lambda_{\rm rot} \geqslant 4\,\epsilon_{\rm soft}$ for $\epsilon_{\rm soft} = 0.01$ and below. The convergence, when $\lambda_{\rm rot}$ is resolved for all particles, is the first suggestion of support for definition of $\lambda_{\rm rot}$ in this environment with disordered motion ($\lambda_{\rm rot} \equiv \pi^2 G\Sigma_{\rm gas}/|\mathbf{\Omega}_{\rm O}|^2$), and is evidence that the minimum requirement to resolve fragmentation at least on the largest scales is to be able to resolve gravity below our definition for the largest unstable scale $\lambda_{\rm rot}$.

In this set of numerical experiments, we resolve fragmentation from the largest unstable scale down to our gravitational resolution. Below the gravitational softening, sub-fragmentation is artificially damped but our aim is to determine if Equation (2) can predict the instability of streams; for this purpose, it is not required to resolve the entire range of unstable wavelengths and

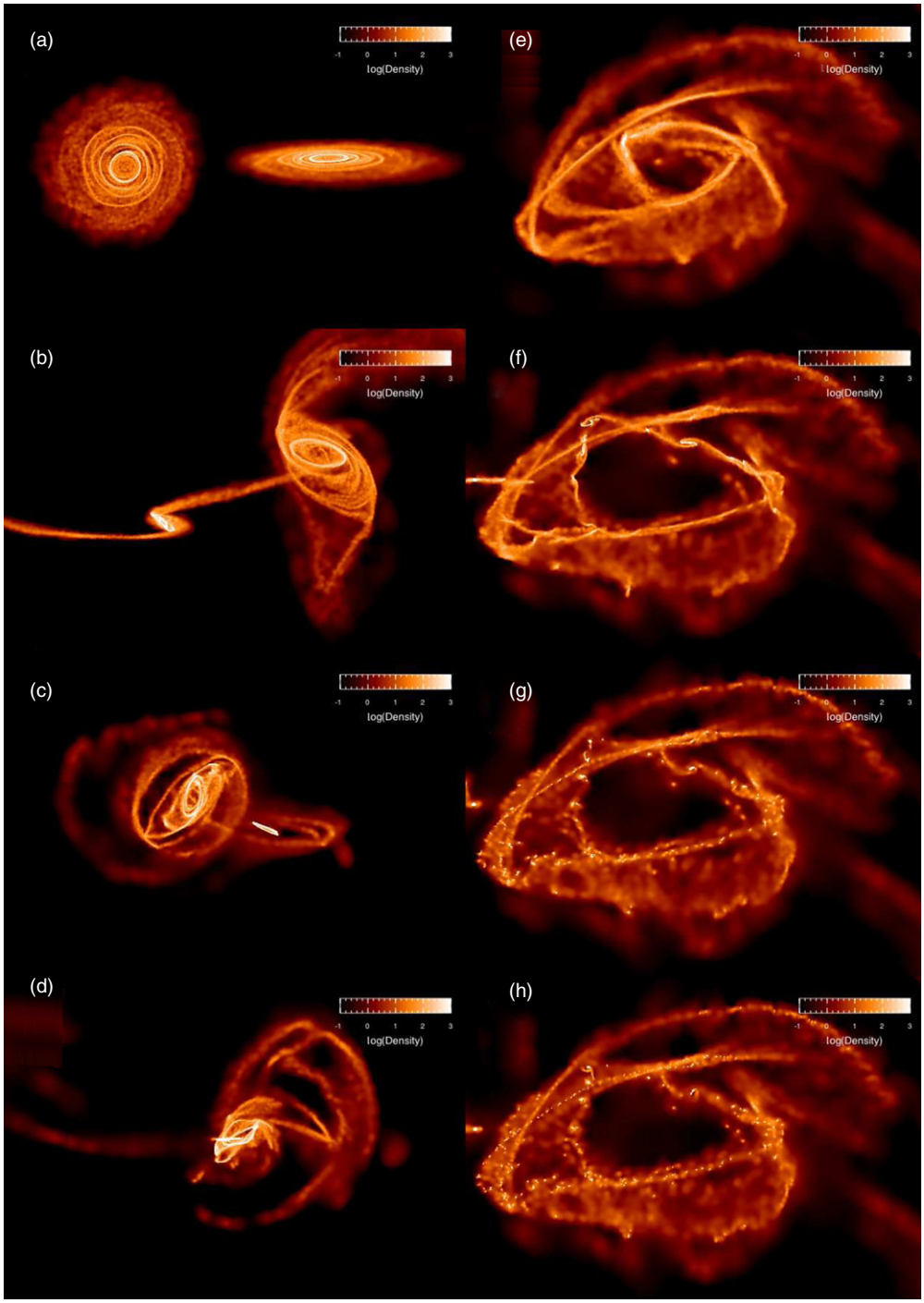

Figure 1. Gas density distribution during the evolution of the galaxy merger shown on a logarithmic scale. Left panels show the density distribution in a box of side 25, in internal units, at the following times: $t = 32$ (a), 54 (b), 120 (c), and 136 (d). Right panels show a zoom-in of the simulation restarted at $t = 132$ (box of side 4 in internal distance units) and evolved up to time $t = 134$ using the following gravitational softening lengths: 0.4 (e), 0.04 (f), 0.01 (g), and 0.006 (h).

(A color version of this figure is available in the online journal.)

it is sufficient that the largest wavelengths are resolved since $\lambda_{\rm rot}/2$ is the first unstable wavelength to appear (i.e., the most unstable mode; Binney & Tremaine 2008).

This resolution test illustrates that, in a set of simulations with the same temperature, fragmentation can be prevented just by the gravitational resolution. This contradicts the interpretation of Teyssier et al. (2010), in which the onset of fragmentation was associated only with a decrease in the temperature. However, Teyssier et al. (2010) changed both temperature and resolution and were unable to disentangle which one (or both) is responsible for the onset of fragmentation. This reinforces our approach of testing the stability criterion (Equation (2)) against a set of simple simulations where the variation of parameters can be fully controlled.

Finally, it is worth mentioning that in this section and in the rest of the paper we will focus only on the fragmentation of the gaseous component. This is because the stellar component behaves approximately as an adiabatic fluid (i.e., the kinetic

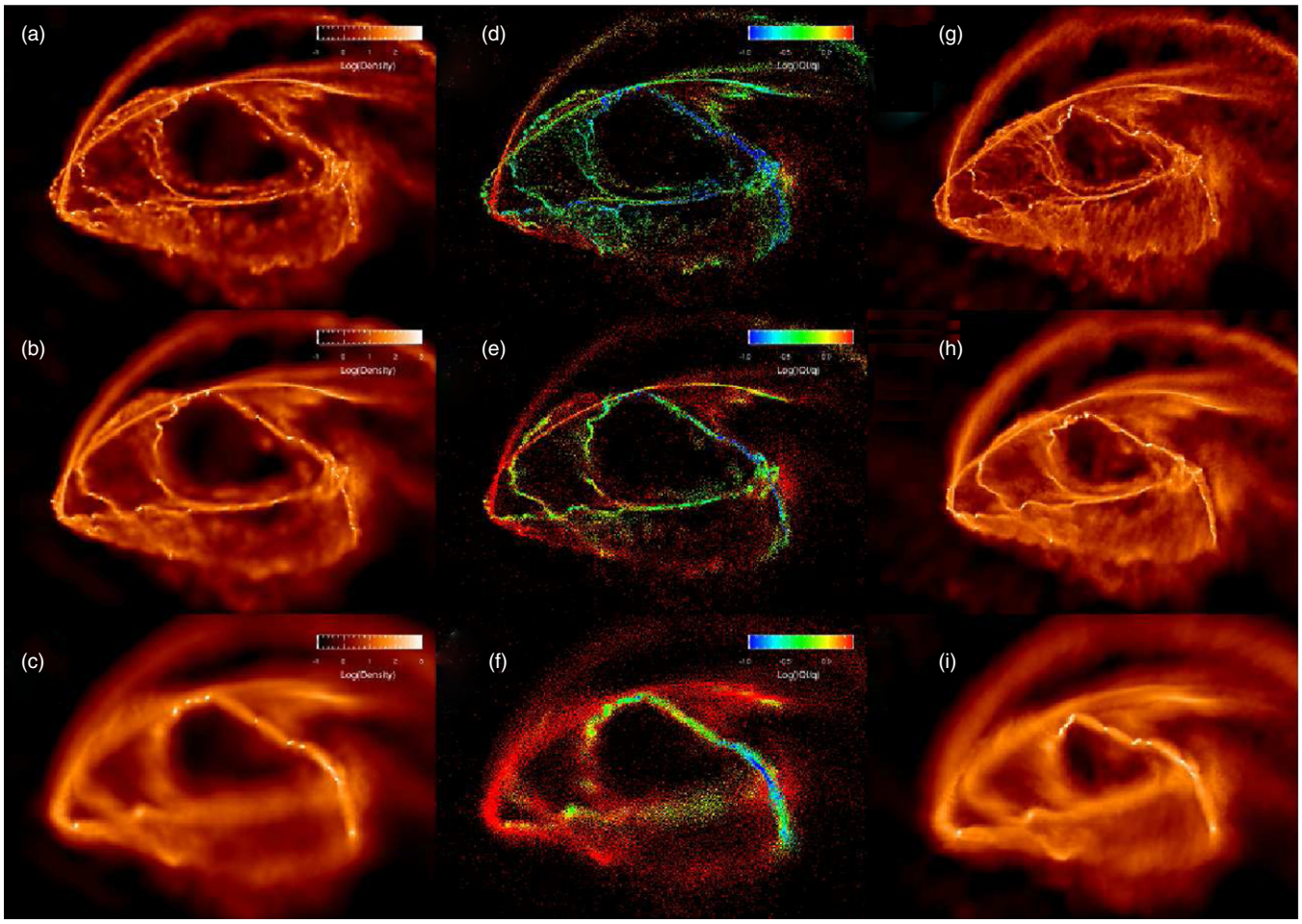

Figure 2. Left panels show the evolution of the gas density distribution at $t = 133.2$ for different temperatures $T = 2 \times 10^4$ (a), 2×10^5 (b), and 10^6 K (c). Middle panels show the predicted $|\boldsymbol{Q}_{\rm O}|/q$ for each particle, computed at the restart time $t = 132$, for the following temperatures: $T = 2 \times 10^4$ (d), 2×10^5 (e), and 10^6 K. (f) Right panels show the evolution of the gas density in the high-resolution runs for different temperatures $T = 2 \times 10^4$ (g), 2×10^5 (h), and 10^6 K (i). In all panels, the boxes have a side of 4 internal distance units.

(A color version of this figure is available in the online journal.)

energy in stellar motion cannot be lost or "radiated" away from the merging system). This leads to a rapid conversion of coherent motion into random motion during the merger, with a subsequent increase of the velocity dispersion in the stellar component, stabilizing the stellar system against runaway fragmentation.

4. TEST OF THE STABILITY CRITERION $|\boldsymbol{Q}_{\rm O}|$

After checking the gravitational resolution needed to resolve fragmentation at least on scales below those of the largest collapsing clumps, we will focus on testing the stability criterion discussed in Section 2 (Equation (2)). Since most of the streams in the inner 2.4 kpc of the system already fragment for $T \sim 2 \times 10^4$ K, we will perform a set of simulations in which we increase the temperature and see how some streams become stable. We will check if the criterion given by Equation (2) successfully predicts if a stream should be stable or not.

Figures 2(a)–(c) show the evolution of the gas density for the system restarted with a gravitational softening length of $\epsilon_{\rm soft} = 0.01$, at $t = 132$, for different temperatures $T = 2 \times 10^4$ (a), 2×10^5 (b), and 10^6 K (c) and evolved to a later time $t = 133.2$. The comparison between different temperatures (Figures 2(a)–(c)) clearly shows that more streams become stable as we increase the temperature.

Figures 2(d)–(f) show $|\boldsymbol{Q}_{\rm O}|/q$ computed for each particle at the time ($t = 132$) at which all the simulations were restarted with $\epsilon_{\rm soft} = 0.01$ for different temperatures $T = 2 \times 10^4$ (d), 2×10^5 (e), and 10^6 K (f). To compute $\boldsymbol{\Omega}_{\rm O}$, we choose as the origin O of the coordinate system the total center of mass (G) of the merging galaxies, because the system as a whole orbits around G and it is also an inertial point for an isolated merger (in the absence of external forces). From Equation (2); the threshold for stability should be around $|\boldsymbol{Q}_{\rm O}|/q = 1$, which corresponds to the yellow particles in Figure 2; the green and blue particles should be unstable and the red ones stable.

The direct comparison of pairs (a) and (d), (b) and (e), and (c) and (f) of Figure 2 shows overall good agreement between the predicted unstable streams (shown in green and blue in Figures 2(d)–(f)) and the streams that eventually fragment on the corresponding Figures 2(a)–(c). In particular, the bluest stream in Figure 2(d) (and in light green in Figure 2(f)) is the most unstable region and the only one that strongly fragments in all simulations (including Figure 2(c)) for temperatures up to 10^6 K.

We find that the stability of gaseous streams is better described for a threshold value $q \sim 0.4$; in fact, we plot $|\boldsymbol{Q}_{\rm O}|/0.4$ in Figures 2(d)–(f). This value of q is approximately a factor of two lower than the value expected for a uniformly rotating isothermal disk ($q = 1.06$; Goldreich & Lynden-Bell 1965). However, it is

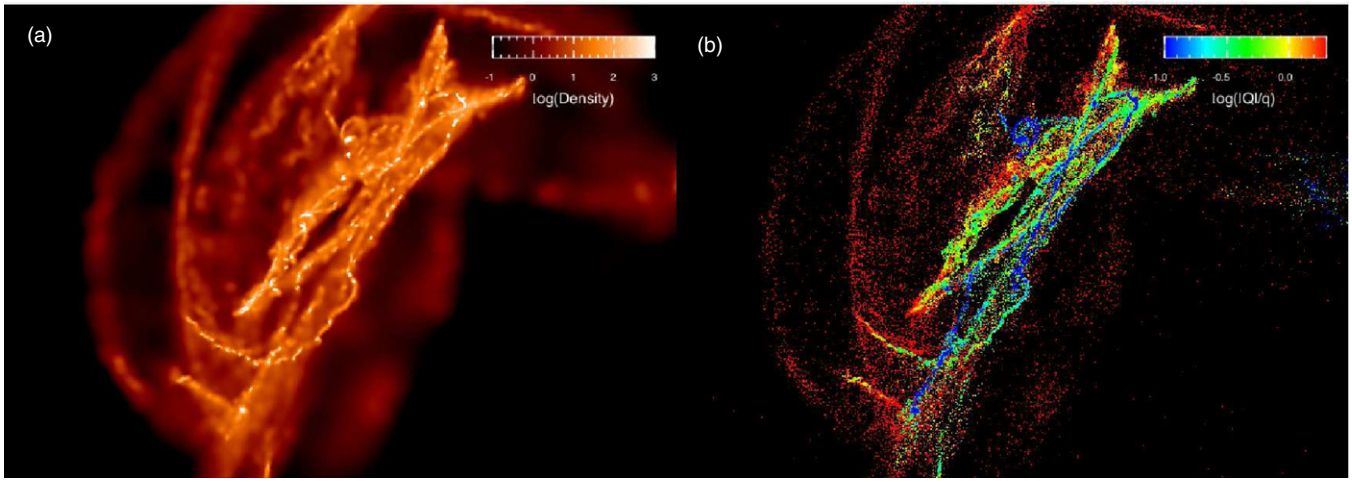

Figure 3. (a) The gas density distribution at $t = 138.4$ of a simulation with a temperature $T = 2 \times 10^4$ K, that was restarted at $t = 137.2$ with a gravitational softening $\epsilon_{\rm soft} = 0.01$. (b) The predicted $|\boldsymbol{Q}_{\rm O}|/q$ for each particle, which is computed at the restarting time $t = 137.2$, for a temperature $T = 2 \times 10^4$ K.
(A color version of this figure is available in the online journal.)

important to emphasize that the actual value of q should depend on the origin O chosen for the coordinates system.

In order to check the numerical reliability of our results, we performed the same fragmentation runs with 2,000,000 gas particles for the different temperatures shown in Figures 2(a)–(c). Figures 2(g)–(i) show the evolution of the gas density for the high-resolution runs. By direct comparison of pairs (a) and (g), (b) and (h), and (c) and (i) of Figure 2, we find differences in the low-density regions, as expected in the SPH technique, and slightly different positions in some streams, also expected due to the different granularity of the gravitational potential. However, we find the same results in terms of the onset of fragmentation of streams (i.e., which ones fragment at a given temperature and which ones do not) and in the number of clumps formed. Therefore, for the purpose of our study, we found consistent results between the low- and high-resolution runs. This supports the reliability of our numerical experiments that test Equation (2).

Finally, it is important to note that although we successfully tested Equation (2) for $t = 132$, it should be valid at any given time for the value of the angular velocity vector at that time (with only with small variations in the threshold q). This is particularly important because, during the evolution of a galaxy merger, the properties of any stream (angular frequency vector, surface density, etc.) can drastically change on a timescale comparable to a crossing time. To check that our criterion is valid at any time, we restarted the original low-resolution simulation again at a different time $t = 137.2$, with a gravitational softening $\epsilon_{\rm soft} = 0.01$ and a temperature $T = 2 \times 10^4$ K.

Figure 3(a) shows the evolution of the gas density for the system restarted at $t = 137.2$ and evolved to a later time $t = 138.4$. Figure 3(b) shows $|\boldsymbol{Q}_{\rm O}|/q$ computed for each particle at the time $t = 137.2$ using the same previously used threshold value $q = 0.4$. The direct comparison of the two sides of Figure 3 again shows overall good agreement between the predicted unstable streams (shown in green and blue in Figure 3(b)) and the streams that eventually fragment in the evolution of the SPH run (Figure 3(a)).

Although the gas properties (and predicted $|\boldsymbol{Q}_{\rm O}|$) at this second restart time have changed considerably compared to the original properties (Figure 2), Figure 3 shows that the $|\boldsymbol{Q}_{\rm O}|$ computed at the restart time $t = 137.2$ successfully predicts which streams will fragment and which ones will not. This is in addition to some minor discrepancies that may arise if we focus on some of the small-scale features shown in Figure 3. For example, a careful inspection of Figure 3(a) shows a smooth spiral pattern around a big clump (slightly up from the center of the image). In the corresponding Figure 3(b), both features are in blue ($|\boldsymbol{Q}_{\rm O}|/q \ll 1$) as expected for the big clump but not for the smooth spiral feature.

Figure 4 shows a zoom-in of such a region: the left panel shows the gas density and the right panel the corresponding $|\boldsymbol{Q}_{\rm O}|/q$. From Figure 4 it is straightforward to realize that the spiral is composed of only a few tens of particles that are lost within the several thousands of particles that compose a clump (i.e., less than 1%). These particles were probably lost through interactions with other clumps and in fact the spiral pattern ends on the closest collapsed clump, suggesting that there are particles lost during strong gravitational interactions between the clumps. These minor discrepancies are inherent to the complexity of the problem, because processes that occur in the subsequent evolution, such as clump–clump interactions, are of course not covered by this or any stability criterion.

In order to quantify these minor discrepancies, we plot in Figure 5 the surface density of each particle against $|\boldsymbol{Q}_{\rm O}|/q$. The left panel of Figure 5 shows the surface density at the restart time $t = 132$ against $|\boldsymbol{Q}_{\rm O}|/q$ computed at the same time. The dashed line represents $\Sigma_{\rm gas} \propto (|\boldsymbol{Q}_{\rm O}|/q)^{-1}$, which gives the overall trend of particles at the restart time. This is expected from the definition given by Equation (2), taking into account that $C_{\rm S}$ is constant and that the dispersion from the overall trend is due to variations of $|\boldsymbol{\Omega}_{\rm O}|$ among particles.

The middle and right panels of Figure 5 show the surface density at $t = 133$ (middle) and $t = 134$ (right) against $|\boldsymbol{Q}_{\rm O}|/q$ computed at the restart time $t = 132$. By construction, the particles in the middle and right panels of Figure 5 can only move in the vertical direction (relative to their position in the left panel) and this will therefore inherently introduce scatter into the $\Sigma_{\rm gas} \propto (|\boldsymbol{Q}_{\rm O}|/q)^{-1}$ trend since the surface density and $|\boldsymbol{Q}_{\rm O}|/q$ are now computed at two different times. As well as the increase in scatter, we see a coherent vertical change for $|\boldsymbol{Q}_{\rm O}|/q \leqslant 1$ as the collapse proceeds. For isothermal simulations like the ones carried out in this work, once the gravitational instability is started it will proceed until the particles reach separations comparable to the softening length

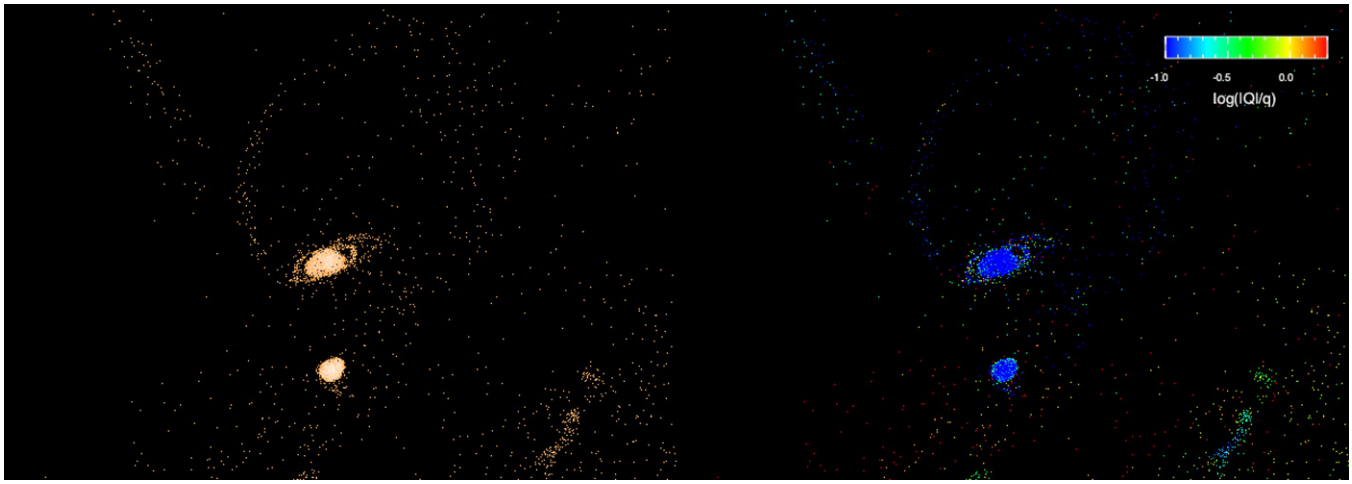

Figure 4. Zoom into the simulation shown in Figure 3. Left: the gas density for each particle at $t = 138.4$. Right: the predicted $|\boldsymbol{Q}_{\rm O}|/q$ for each particle, which is computed at the restart time $t = 137.2$.

(A color version of this figure is available in the online journal.)

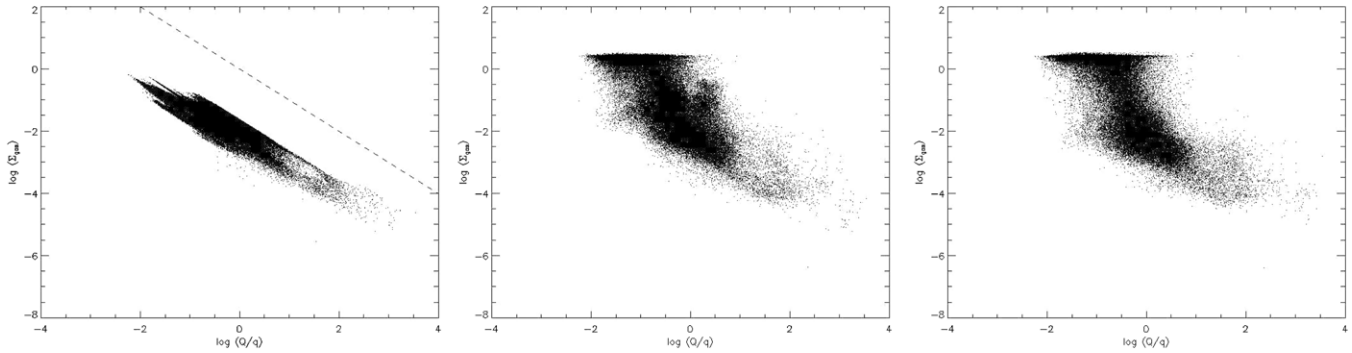

Figure 5. Evolution of the surface density as fragmentation proceeds. The predicted $|\boldsymbol{Q}_{\rm O}|/q$ for each SPH particle, computed at the restart time $t = 132$, is plotted against the surface density of each particle at time $t = 132$ (left), $t = 133$ (middle), and $t = 134$ (right). The dashed line in the left panel represents $\Sigma_{\rm gas} \propto (|\boldsymbol{Q}_{\rm O}|/q)^{-1}$, which is the overall trend of particles at the restart time $t = 132$.

and this behavior happens regardless of the $|\boldsymbol{Q}_{\rm O}|/q$ or $\Sigma_{\rm gas}$ values. The horizontal saturated region in the middle and right panels of Figure 5 (at $\log(\Sigma_{\rm gas}) \geqslant 0$) shows this behavior. On the other hand, the time to move to the saturated region (the free-fall time) does depend on $\Sigma_{\rm gas}$ and this explains why the dark region of particles with $\log(\Sigma_{\rm gas}) \leqslant 0$ recedes toward higher $|\boldsymbol{Q}_{\rm O}|/q$ as times evolves (from $\log(|\boldsymbol{Q}_{\rm O}|/q) \geqslant -1.5$ in the middle panel to $\log(|\boldsymbol{Q}_{\rm O}|/q) \geqslant -1$ in the right panel of Figure 5).

In the right panel of Figure 5, the particles in the region $\log(\Sigma_{\rm gas}) \leqslant 0$ and $\log(|\boldsymbol{Q}_{\rm O}|/q) \leqslant -1$ are representative of particles lost from the collapsing clumps, like the ones shown in the spiral feature of Figure 4. In the same way, the particles in the region $\log(\Sigma_{\rm gas}) \geqslant 0$ and $\log(|\boldsymbol{Q}_{\rm O}|/q) \geqslant 0$ represent particles from stable regions that are gravitationally captured by the collapsing clumps. Despite these departures, the overall trend is clear and shown in the right panel of Figure 5, where a drastic change at $\log(|\boldsymbol{Q}_{\rm O}|/q) = 0$ is clearly seen; this is due to the collapse of the unstable regions, which moves their particles vertically up, producing the horizontal saturated region seen for $\log(|\boldsymbol{Q}_{\rm O}|/q) \leqslant 0$.

5. SUMMARY

In this paper, we have studied the gravitational stability of gaseous streams in the complex environment of a galaxy merger using hydrodynamic simulations.

We find that the stability parameter of a rotating annulus can be generalized to study the problem of multiple gaseous streams orbiting around the merger remnant by using the angular frequency vector of each stream. This approximation should be valid as long as the orbital motion of a stream can be well approximated by the rotational motion around the center of gravity on a given plane, which is what happens in the inner regions of the merger remnant.

We test our generalized stability criterion, $|\boldsymbol{Q}_{\rm O}| \geqslant q$, using SPH numerical simulations specially designed for that purpose. We find that this criterion successfully predicts the streams that will be gravitationally unstable to fragmentation into clumps. In our simulations, we find that the stability of streams is better described by choosing a threshold value $q \sim 0.4$.

The generalization of $\lambda_{\rm rot}$ in a galaxy merger is also relevant for the formation of massive globular-type clusters since its associated mass $M_{\rm rot} = \Sigma_{\rm gas}\,(\lambda_{\rm rot}/2)^2$ is related to the characteristic mass of the most massive clusters that are able to form (Escala & Larson 2008; Shapiro et al. 2010) and has a role in the triggering of star formation, since it correlates with the galactic star formation rate (Escala 2011).

The numerical validation of stability for $|\boldsymbol{Q}_{\rm O}| \geqslant q$ opens new possibilities for future research. One of these is to apply the criterion given by Equation (2) to observations of gas-rich galaxy mergers and also to simulations with a more realistic description for the ISM that includes feedback processes from

star formation and/or AGNs. Another interesting possibility is to study when in the evolution of a merger, a larger portion of the gaseous mass has $|\boldsymbol{Q}_{\rm O}| \leqslant q$ and then to determine when in a galaxy merger the streams would fragment more vigorously.

A.E. acknowledges partial support from the Center for Astrophysics and Associated Technologies CATA (PFB 06) and Anillo de Ciencia y Tecnología ACT1101. F.B. and L.d.V. acknowledge support from Programa Nacional de Becas de Postgrado (Grant D-22100632 and Grant D-21090518). The simulations were performed using the HPC clusters Markarian (FONDECYT 11090216), Geryon (PFB 06), and Levque (ECM-02).

REFERENCES

Barnes, J. E., & Hernquist, L. 1996, ApJ, 471, 115
Binney, J., & Tremaine, S. 2008, Galactic Dynamics (Princeton, NJ: Princeton Univ. Press)
Bonnor, W. B. 1956, MNRAS, 116, 351
Bournaud, F., Duc, P.-A., & Emsellem, E. 2008, MNRAS, 389, 8
Chandrasekhar, S., & Fermi, E. 1953, ApJ, 118, 116
Cox, T. J., Dutta, S. N., Di Matteo, T., et al. 2006, ApJ, 650, 791
Di Matteo, P., Combes, F., Melchior, A.-L., & Semelin, B. 2007, A&A, 468, 61
Ebert, R. 1955, ZA, 37, 217
Escala, A. 2011, ApJ, 735, 56
Escala, A., & Larson, R. B. 2008, ApJ, 685, L31
Goldreich, P., & Lynden-Bell, D. 1965, MNRAS, 130, 97
Jeans, J. H. 1902, RSPTA, 199, 1
Kazantzidis, S., Mayer, L., Colpi, M., et al. 2005, ApJ, 623, 67
Kuijken, K., & Dubinski, J. 1995, MNRAS, 277, 1341
Larson, R. B., & Tinsley, B. M. 1978, ApJ, 219, 46
Matsui, H., Saitoh, T. R., Makino, J., et al. 2012, ApJ, 746, 26
Mengel, S., Lehnert, M. D., Thatte, N. A., et al. 2008, A&A, 489, 1091
Mihos, J. C., & Hernquist, L. 1994, ApJ, 431, 9
Mihos, J. C., & Hernquist, L. 1996, ApJ, 464, 641
Saitoh, T., Daisaka, H., Kokubo, E., et al. 2009, PASJ, 61, 481
Sanders, D. B., & Mirabel, I. F. 1996, ARA&A, 34, 749
Schwarz, M. P. 1984, MNRAS, 209, 93
Schweizer, F., & Seitzer, P. 1998, AJ, 116, 2206
Shapiro, K. L., Genzel, R., & Förster Schreiber, N. M. 2010, MNRAS, 403L, 36
Springel, V. 2005, MNRAS, 364, 1105
Teyssier, R., Chapon, D., & Bournaud, F. 2010, ApJ, 720, 149
Toomre, A. 1964, ApJ, 139, 1217
Toomre, A., & Toomre, J. 1972, ApJ, 178, 623